ISSN: 1410-8917
e-ISSN: 2597-9914

Jurnal Kimia Sains dan Aplikasi 23 (2) (2020): 39–45

Jurnal Kimia Sains dan Aplikasi
Journal of Scientific and Applied Chemistry

Journal homepage: http://ejournal.undip.ac.id/index.php/ksa

Utilization of Coconut Shell as Cr_2O_3 Catalyst Support for Catalytic Cracking of Jatropha Oil into Biofuel

Isalmi Aziz [a,*], Yessinta Kurnianti [a], Nanda Saridewi [b], Lisa Adhani [c], Wahyu Permata [d]

[a] Chemistry Study Program, UIN Syarif Hidayatullah Jakarta, South Tangerang, Banten, Indonesia
[b] Chemistry Education Study Program, UIN Syarif Hidayatullah Jakarta, South Tangerang, Banten, Indonesia
[c] Department of Chemical Engineering, Bayangkara University, Bekasi, West Java, Indonesia
[d] Environmental Laboratory, UIN Syarif Hidayatullah Jakarta, South Tangerang, Banten, Indonesia

*Corresponding author: isalmikimia@uinjkt.ac.id

https://doi.org/10.14710/jksa.23.2.39-45

Article Info

Article history:

Received: 3rd December 2019
Revised: 20th January 2020
Accepted: 17th February 2020
Online: 29th February 2020

Keywords:
Coconut shell; carbon; catalytic cracking; biofuel; gasoline

Abstract

Coconut shell waste is a waste that has a high carbon content. Carbon in coconut shell waste can be converted into activated carbon having a large surface area. This potential property is suitable to apply the coconut shell as catalyst support. To increase the catalytic activity, metal oxides such as Cr_2O_3 are impregnated. The purpose of this study is to synthesize Cr_2O_3/carbon catalyst and test its catalytic activity on catalytic cracking of Jatropha oil. The first stage was the synthesis of activated carbon and the determination of its proximate and ultimate. The second step was impregnation to produce Cr_2O_3/carbon catalyst. Furthermore, X-Ray Diffraction to determine crystallinity, Surface Area Analyzer to identify its surface area and Fourier Transform Infrared to analyze functional groups. Then the catalytic activity was tested on the catalytic cracking of Jatropha oil. In addition, the chemical compound composition and biofuel selectivity of the catalytic cracking product was determined using Gas Chromatography-Mass Spectrometer. Proximate analysis results showed that activated carbon contains 9%, 1%, 23%, and 67% of water, ash, evaporated substances, and bound carbon, respectively. The results of the ultimate analysis resulted in carbon (C), hydrogen (H), and nitrogen (N) contents of 65.422%, 3.384%, and 0.465%, correspondingly. The catalyst crystallinity test showed the presence of Cr_2O_3 peaks at 2θ: 24.43°; 33.47° and 36.25° according to JCPDS No. 84-1616. In the absorption area of 400-1000 cm^{-1} and the range of 2000 cm^{-1} showed the presence of Cr-O stretching due to Cr_2O_3 adsorbed into the activated carbon structure. The surface area of activated carbon and Cr_2O_3/carbon catalysts with a concentration of 1.3, and 5% was 8.930 m^2/g; 47.205 m^2/g; 50.562 m^2/g; and 38.931 m^2/g, respectively. The catalytic activity test presented that the best performance was showed by Cr_2O_3/carbon catalyst with a concentration of 5% indicated by conversion of Jatropha oil into biofuel of 67.777% with gasoline selectivity, kerosene, and diesel of 36.97%, 14.87%, and 15.94%, correspondingly.

1. Introduction

Biofuel is alternative energy to substitute petroleum sourced from vegetable or animal material. *Jatropha curcas* oil is one of the most potential vegetable materials used as raw material for biofuel production because it is easily produced and non-edible. The oil content in the castor bean core is around 50% [1]. Jatropha oil contains 16-18 carbon atoms in each molecule, while petroleum contains 8-10 carbon atoms (gasoline) and 12-18 carbon atoms (diesel). The higher carbon atom content of Jatropha oil results in higher viscosity (thicker) when compared to petroleum viscosity [2]. For this reason, a process which enables to reduce the number of carbon atoms from Jatropha oil is necessary.

Conversion of Jatropha oil into biofuel can be carried out by catalytic cracking. Catalytic cracking is the process

of terminating a heavy fraction compound into a mild fraction with the help of a catalyst. The catalyst customarily applied is heterogeneous because it is easy to separate from the product and can be regenerated. Aziz *et al.* [3] used natural zeolite as a catalyst in catalytic cracking of *Jatropha curcas* oil (*Jatropha curcas* L) into biofuel. The optimum process conditions were obtained at 375°C, 2 hours, a catalyst with a size of 180 µm and 5% concentration with selectivity to gasoline 34.52%, kerosene 11.87%, and diesel 13.64%. Meanwhile, Novia *et al.* [2] used a Co/Mo Montmorillonite pillared TiO_2 catalyst in castor oil hydrocracking. The yield of the product is 77.7127% at a temperature of 500°C, a gas flow rate of 2.5 mL/s, and 2 grams of the amount of catalyst.

The function of zeolites and TiO_2 is a catalyst supports. Zeolites are minerals in nature that are of limited availability. Likewise, TiO_2 is a synthetic compound, and the price is high. Another type of catalyst support that can be applied is activated carbon since it has a large surface area of around 300-3500 m^2/g [4]. A large surface area will affect the rate of reaction. The greater the surface area of the catalyst, the higher the reaction rate.

In this study, the raw material used for the manufacture of activated carbon came from coconut shell waste. So far, coconut shells have only been used as briquettes [5, 6, 7] or adsorbents [8, 9]. Conversion of coconut shell to activated carbon (catalyst support) increases the economic value of the coconut shell. It also reduces the cost of biofuel production when using a coconut shell as catalyst support. Kurniawan *et al.* [4] synthesized activated carbon from coconut shells with activation using 3M phosphoric acid, producing a surface area of 386.447 m^2/g. Ain *et al.* [10] used activated carbon (synthetic) as a buffer for the Ru-Sn/C catalyst for the hydrogenation of hexadecanoic acid to 1-hexadecanol. The advantages of activated carbon as a supported catalyst are a large surface area, resistant to acids, stable at high temperatures, and inert [11]. The active catalyst components used are usually derived from transition metals such as Cr, Ni, Mo [12], Pd [13], and Fe [14] because they have vacant d orbitals. The presence of vacant d orbitals allows the availability of Lewis acid groups so that they can provide an active site of the catalyst [15]. In this study, chromium was used because it had higher acidity, smaller pore size, and high surface area [16].

This research varied the concentration of Cr_2O_3 impregnated into activated carbon by 1, 3, and 5%. The characteristics of the resulting catalysts were analyzed using X-Ray Diffraction (XRD), Fourier Transform Infrared (FTIR), and Surface Area Analyzer (SAA). The catalytic activity test was conducted in a reactor batch at 375°C for 5 hours. The resulting product was then analyzed its chemical composition using Gas Chromatography-Mass Spectroscopy (GC-MS) to determine the conversion and selectivity of the resulting biofuel.

2. Materials and Methods

2.1. Equipment and Materials

The equipment used consisted of a glass (pyrex), a grinding mill, a set of reactor batch (stainless steel), a LECO CHN628 ultimate analyzer, a Gas Chromatography-Mass Spectrometer (GC-MS) Shimadzu QP 2010, a X-Ray Diffraction (XRD) Rigaku Mini Flex 600, a Fourier Transform Infrared (FTIR) Shimadzu, and a Quantachrome NovaWin's Surface Area Analyzer (SAA). The materials used were coconut shell waste obtained from the Cipete Block A Market, South Jakarta, Jatropha oil (Hensa Kimia), H_3PO_4 (Merck, 85%), Cr $(NO_3)_3.9H_2O$ (Merck, 99.99%), distilled water and ethanol (70%).

2.2. Synthesis of Activated Carbon

The coconut shell was cleaned from dirt and cut into smaller sizes. After that, it was put into the furnace for carbonization to be carried out at a temperature of 450°C for 2 hours. The resulting carbon was crushed until smooth and soaked in 300 mL of 3M phosphoric acid (H_3PO_4) solution for 7 hours. Activated carbon was then washed with hot water till neutral pH was achieved and then dried [4]. The activated carbon produced was tested for proximate analysis, including water, ash, volatile substances, bound carbon, and ultimate analysis, including C, H, and N contents.

2.3. Production of Cr_2O_3/carbon catalysts

Chromium nitrate ($Cr(NO_3)_3.9H_2O$) divided into three parts with a different mass that was 1.576; 4.738 and 7.890 grams were dissolved in 20 mL distilled water and stirred until homogeneous. Every sample was then added activated carbon (28.423; 25.261 and 22.109 grams), stirred at 60° C for 3 hours and evaporated. The sample was then dried at 120°C in the oven and then calcined at 450°C for 1 hour to produce a Cr_2O_3/carbon catalyst.

2.4. Catalyst Characterization

Surface area analysis was carried out using the Surface Area Analyzer (SAA). 0.1 gram of sample was put in an empty tube then degassing for 2 hours at 200 °C while flowing 275 KPa of N_2 gas and cooled. After degassing, the sample was analyzed immediately. N_2 gas flowed at 275 KPa and 20 Psi H_2 gas. The analysis conditions were then adjusted. The analysis time was around ± 5 hours per sample. The catalyst crystallinity test uses X-Ray Diffraction (XRD). The crystallinity test was carried out at a voltage of 40 kV and a current of 25 mA with an angular range of 5-90°. The identification of functional groups was conducted using Fourier Transform Infrared (FTIR). Samples were mashed together with KBr in a ratio of 1:10 and measured at wavelengths of 500–4000 cm^{-1}.

2.5. Catalyst Activity Test on Jatropha Oil Cracking Catalytic

10 mL of *Jatropha curcas* oil and 0.5 gram of Cr_2O_3/carbon catalyst were put into the reactor batch. The reactor heater was run to 375°C, then the stirrer was ignited, and the reaction time was calculated for 5 hours.

The product was removed from the reactor and separated from the catalyst.

2.6. Analysis of Jatropha Cracking Catalytic Cracking Products

Catalytic cracking products of *Jatropha curcas* oil were tested for their chemical composition using Gas Chromatography-Mass Spectrometer (GC-MS). A sample of 1 µL was injected into the column (DB5-MS UI stationary phase, 30 m; 0.25 mm; 0.25 µm and Helium gas mobile phase). The resulting chromatogram data were then compared with the standards database so that the chemical compounds produced can be determined. From the product area data produced, product selectivity can be calculated for each Cr_2O_3/carbon catalyst. Biofuel selectivity is calculated using the formula [17]:

$$Selectivity = \frac{Area\ of\ biofuel}{Total\ of\ product\ area} x\ 100\% \quad (1)$$

3. Results and Discussion

3.1. Results Analysis of Proximate and Ultimate of Activated Carbon

Table 1 shows the results of the proximate analysis of activated carbon. The water content contained in activated carbon is 9.756% smaller than the maximum limit stipulated by SNI 06-3730-1905. In addition, ash and volatile substance contents are 0.961%, 22.660%, respectively. The bound carbon content is 66.662% greater than the minimum limit stipulated by SNI. These results show that the activated carbon produced meets SNI 06-3730-1905 standards. The value of bound carbon content is inverse with the content of ash, water, and volatile substances. This indicated that the surface of activated carbon became more open because the impurities that cover the surface of the activated carbon are released so that the surface area becomes larger [18].

Table 1. Result analysis of proximate of activated carbon

Parameter	Content (%)	SNI 06-3730-1995 (%)
Water	9.756	Max. 15
Ash	0.961	Max. 10
Volatile substances	22.660	Max. 25
Bound carbon	66.623	Min. 65

The ultimate analysis results, as listed in Table 2, show carbon (C) content of 65.422%, hydrogen 3.384%, and nitrogen 0.465%. This result also shows that the quality of activated carbon produced meets SNI standards that require a minimum carbon content of 65%. The ultimate analysis results for carbon content are in line with the bound carbon levels produced in the proximate analysis.

Table 2. Result of the ultimate of activated carbon

Element	Content (%)
C	65.422
H	3.384
N	0.465

3.2. Characterization of Cr_2O_3/Carbon Catalyst

Figure 1 shows the XRD patterns of activated carbon and Cr_2O_3/carbon catalysts at concentrations of 1%, 3%, and 5%. The activated carbon produced has an irregular shape, and there are no sharp peaks. This shows that activated carbon has an amorphous phase [19]. A wide-angle range and a soft peak in the range of 24° indicate the phase for activated carbon [20]. The Cr_2O_3/carbon XRD patterns show Cr_2O_3 peaks at 2θ 24.52°; 33.61°; 36.25° with hkl index (012, 104 and 110) according to JCPDS No. 84-1616. The peaks at 2θ 24°; 33°; and 36° are the typical peaks for Cr_2O_3 [21, 22]. The peaks are not very clearly seen because the amorphous phase of carbon is more dominant, but as shown in Table 3, it appears that the increase in Cr_2O_3 concentration increases the intensity of the peaks.

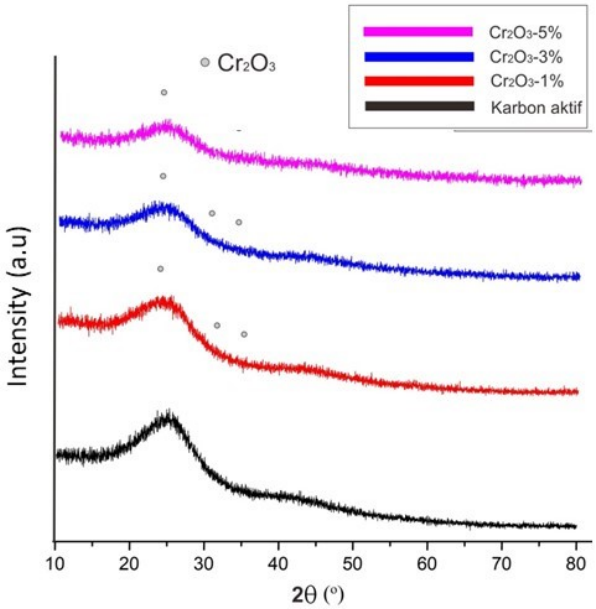

Figure 1. X-ray diffractogram of activated carbon and Cr_2O_3/carbon catalysts of 1%, 3%, and 5%

Table 3. Peak intensity of Cr_2O_3/carbon catalyst

Cr_2O_3/carbon 1%		Cr_2O_3/carbon 3%		Cr_2O_3/carbon 5%	
2θ (°)	Intensity	2θ (°)	Intensity	2θ (°)	Intensity
24.27°	10.0	24.80°	292.6	24.43°	422.9
33.61°	6.1	33.46°	179.5	33.47°	259.4
36.21°	2.7	36.20°	78.1	36.25°	112.9

Figure 2 shows the FTIR spectra of activated carbon and Cr_2O_3/carbon catalysts. In activated carbon, wave number at 3637.75 cm^{-1} shows the most massive absorption band of the hydroxyl group (O-H). Septiani *et al.* [19] also stated that the hydroxyl group (O-H) appeared in the region of the 3300-3399 cm-1 wave range assigned as the Bronsted acid site. In addition, there is also a carbonyl group (C=O) observed at 1716.65 cm^{-1}. Mentari *et al.* [23] stated that the absorption peak at 1820-1600 cm^{-1} indicates the presence of the C=O group, where this group is a typical group present in activated carbon. Moreover, the peak observed at 1591.27 cm^{-1} indicates the presence of an aromatic group (C=C). The presence of the C=C group shows high carbon content.

The absence of significant changes in the position of the absorption band indicates the impregnation of Cr_2O_3 into activated carbon, but there was a slight shift in the absorption band at 400-1000 cm^{-1} and 2000 cm^{-1}. This shift is due to Cr_2O_3 adsorbed into activated carbon. Cr_2O_3/carbon catalyst spectra of 1%, 3%, and 5% lead to the presence of new absorption around 800 cm^{-1}. Rahmani *et al.* [24] stated that the addition of the transition metal into the material support only causes a slight change in the position of the absorption band. The new peak is also observed at of 2054.19 cm^{-1}; 2027.19 cm^{-1}; 2002.11 cm^{-1} attributed to the Cr-O vibration coming from Cr_2O_3. In addition, the appearance of weak absorption peaks in regions 570 and ~ 635 shows typical absorption peaks for the vibrations of Cr_2O_3 metal oxides [21, 25].

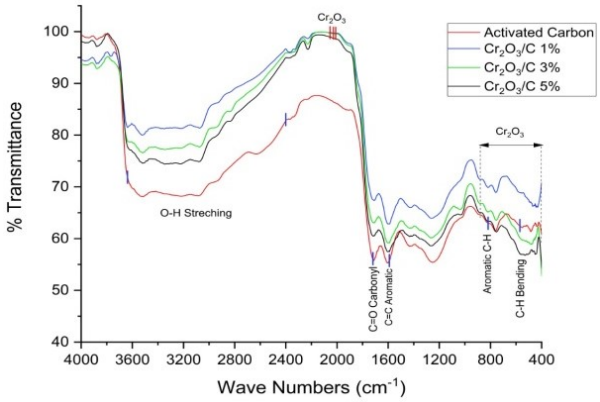

Figure 2. FTIR spectra of activated carbon and Cr_2O_3/carbon catalysts of 1%, 3% dan 5%

The surface area of activated carbon and catalysts produced can be seen in Table 4. Activated carbon has a surface area of 8.930 m^2/g while Cr_2O_3/carbon catalysts of 1%, 3%, and 5% produced a surface area of 47.205 m^2/g; 50.562 m^2/g; and 38.931 m^2/g. Cr_2O_3 impregnation on the surface of the activated carbon buffer increased the catalyst surface area. This happened because the Cr_2O_3 particles entered into the activated carbon pores, so they are well supported. This resulted in the interaction between Cr_2O_3, which acts as an active component providing the catalyst active site and the reactants occurred more quickly.

Fanani *et al.* [26] also found an increase in the surface area of the catalyst when Cr was applied to activated carbon. The area of activated carbon with the addition of chromium metal increased from 1527.80 m^2/g to 1652.58 m^2/g. According to Lillo-Ródenas *et al.* [27], the increase of the catalyst surface area is due to the pores becoming more open after chemical activation and impregnation of the metal led to the surface area of the catalyst became larger. The increase in the surface area occurs at a concentration of 1% to 3%. The surface area of the catalyst represents the active surface, which can interact with the reactants. The reactant molecule will move freely before experiencing adsorption on the surface of the catalyst, then reacts to generate a product.

The surface area of 5% Cr_2O_3/carbon catalyst is 38.931 m^2/g smaller than 1% and 3% Cr_2O_3/carbon catalysts. This is due to the addition of more metal concentration resulted in competition among the transitions metals to diffuse into the supporting pores [28]. It also can be caused by the high concentration of Cr_2O_3, leading to an agglomeration of metal oxide particles; as a result, the formation of unevenly distributed aggregate on the pore surfaces thereby reducing the surface area [29].

Table 4. The surface area of activated carbon and Cr_2O_3/carbon catalysts

Catalyst	Surface area (m2/g)
Activated carbon	8.930
Cr_2O_3/carbon 1%	47.205
Cr_2O_3/carbon 3%	50.562
Cr_2O_3/carbon 5%	38.931

3.3. Cr_2O_3/carbon catalyst activity test

The results of GC-MS analysis show that the Jatropha oil fatty acid constituents used as raw material for making biofuels can be seen in Table 5 and Figure 3.

Table 5. Composition of fatty acid in Jatropha oil

Peak no	Retention time (minutes)	Component	Area percentage (%)
1	19.342	Palmitic acid (C16:0)	9.84
2	21.714	Linoleic acid (C18:2)	33.83
3	21.816	Oleic acid (C18:1)	37.44
4	22.188	Stearic acid (C18:0)	15.59
5	24.467	Eocosenoic acid (C20:1)	3.30

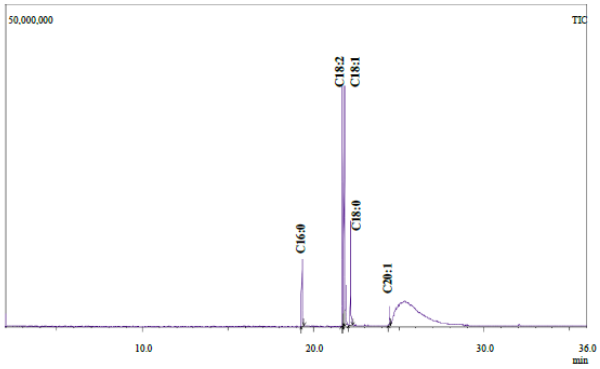

Figure 3. Chromatograms of fence castor oil

In Table 5, it can be seen that fatty acids containing in Jatropha oil consist of palmitic acid, linoleic acid, oleic acid, stearic acid, and eicosuric acid with the value of 9.88%, 33.83%, 37.44%, 15.59%, and 3.30%, respectively. Most of them are unsaturated fatty acids, i.e., oleic and linoleic acids. Weinert *et al.* [30] stated that the most fatty acids containing in Jatropha oil were unsaturated fatty acids 76.8% while saturated fatty acids were 23.2%. After catalytic cracking using a Cr_2O_3/carbon catalyst 1%, 3%, and 5%, the results obtained are as shown in Table 6.

Table 6. Composition of catalytic cracking products of fence castor oil

Product	Composition (%)		
	Cr_2O_3/carbon 1%	Cr_2O_3/carbon 3%	Cr_2O_3/carbon 5%
Hydrocarbon (biofuel, %)	51.82	60.10	68.13
Fatty acid (%)	40.10	31.18	31.77

In Table 6, it can be seen that the two largest classes of compounds produced from catalytic cracking of fence castor oil consist of hydrocarbons (biofuels) and fatty acids. The hydrocarbons produced vary from C_5 to C_{20}. These hydrocarbons are biofuel compounds (the desired products of this reaction). The types of fatty acids produced from the three types of catalysts are different from the constituents of castor oil, including heptanoic acid, octanoic acid, and others. These show that all fatty acids from castor oil can be converted into biofuels and fatty acids with shorter carbon chains.

Of all the products available, all of them are new compounds; these show that all reactants (Jatropha oil) can be converted 100% into products (hydrocarbons and fatty acids). The greater the concentration of Cr_2O_3 impregnated into the supporting material, the greater the conversion (Table 5). Cr_2O_3/carbon 1%, Cr_2O_3/carbon 3% and Cr_2O_3/carbon 5% catalysts resulted in conversion of Jatropha oil to biofuel at 58.55%, 60.10% and 67.77%, respectively. This is also in agreement with the selectivity of the resulting biofuel fraction. The increase in Cr_2O_3 concentration caused the selectivity of light fractions (gasoline) to increase (Table 7). The more light fraction content in biofuels, indicating the catalytic cracking process was running optimally. This also proves that the Cr_2O_3/carbon catalyst has a good cracking ability in breaking the heavy fraction (castor oil) into the light fraction (gasoline). So it can be concluded that the Cr_2O_3/carbon 5% catalyst showed the best results with the conversion of castor oil into biofuel by 67.77% and 36.961% gasoline selectivity; 14.875% kerosene and 15.941% diesel.

Table 7. The selectivity of biofuel product

Catalyst	Selectivity (%)		
	Gasoline	Kerosene	Diesel
Cr_2O_3/carbon 1%	24.748	14.061	13.014
Cr_2O_3/carbon 3%	30.626	14.597	15.223
Cr_2O_3/carbon 5%	36.961	14.875	15.941

Catalytic cracking of fence Jatropha oil can occur through 2 stages, namely the formation of oxygenated components such as fatty acids, ketones, aldehydes, esters, and others caused by the decomposition of triglyceride molecules [28]. These are evidenced by the presence of fatty acids in fence Jatropha oil cracking results. The reaction is as follows:

$$\text{Triglyceride} \xrightarrow{H^+} R_1COOH + R_2CH_2CH_3 + R_3COOCH_3 + CO_2$$

The second stage is indicated by cracking oxygenated components to form hydrocarbons [31]. Oxygenated compounds will break the C-O and C-C bonds by breaking the carbon chain at the beta position. Breaking of the C-O and C-C bonds through 2 reaction routes i.e., the decarboxylation and the decarbonation reactions. Decarboxylation reaction is a reaction to break the carboxylic bonds to produce CO_2 gas and hydrocarbons [32]. Decarboxylation reaction example in *Jatropha curcas* oil is the conversion of stearic acid becomes heptadecane by cracking process as follows:

$$C_{17}H_{35}COOH \rightarrow C_{17}H_{36} + CO_2$$

Decarbonylation reaction is a reaction indicating the release of the ester group to produce hydrocarbons, CO, and H_2O. Decarbonylation reaction example is the decomposition of undecanoic acid to decane (cracking results) as follows:

$$C_{11}H_{22}O_2 \rightarrow C_{10}H_{20} + H_2O + CO$$

4. Conclusion

Activated carbon from coconut shell waste can be used as a Cr_2O_3/carbon catalyst supporting material. The XRD pattern of the catalyst showed typical peaks of Cr_2O_3 observed at 2θ 24.52°; 33.61°; 36.25°. The vibration modes observed at 400-1000 cm^{-1} and 2000 cm^{-1} indicate the presence of Cr-O stretching due to Cr_2O_3 adsorbed into activated carbon. The surface area of activated carbon is 8.930 m^2/g while the Cr_2O_3 catalyst 1%, 3%, and 5% are 47.205 m^2/g; 50.562 m^2/g; and 38.931 m^2/g. The best catalytic activity test shows the best concentration of Cr_2O_3/activated carbon catalyst is 5% with the conversion of castor oil to 67.777% biofuel, 36.97% gasoline selectivity, 14.87% kerosene, and 15.94% diesel.

Acknowledgment

The author would like to thank the Research and Publishing Center (Puslitpen) UIN Syarif Hidayatullah Jakarta for funding this research through SK Rektor No. Un.01/KPA/510/2019 for Higher Education Development Research.

References

[1] Roni Assafaat Hadi, 2019, Keragaan Pertumbuhan Tanaman Jarak Pagar (*Jatropha curcass*) di Pembibitan Akibat Pemberian Mikoriza di Dua Lokasi Berbeda Berdasarkan Ketinggian Tempat, *Jurnal Pertanian*, 10, 1, 43-51 http://dx.doi.org/10.30997/jp.v10i1.1655

[2] Novia, Kachairisma, Lidya Anggraini, 2011, Pembuatan Bio-Gasolin dari Minyak Jarak Pagar Melalui Proses Hydrocracking, *Jurnal Teknik Kimia*, 17, 5, 50-58

[3] I. Aziz, L. Adhani, T. Yolanda, N. Saridewi, 2019, Catalytic cracking of *Jatropa curcas* oil using natural zeolite of Lampung as a catalyst, *IOP Conference Series: Earth and Environmental Science*, 299, 012065 https://doi.org/10.1088/1755-1315/299/1/012065

[4] Riski Kurniawan, Musthofa Lutfi, Wahyunanto Agung Nugroho, 2013, Karakterisasi luas permukaan bet (braunanear, emmelt dan teller) karbon aktif dari tempurung kelapa dan tandan kosong kelapa sawit dengan aktivasi asam fosfat (H_3PO_4), *Jurnal Keteknikan Pertanian Tropis dan Biosistem*, 2, 1, 15-20

[5] Didi Dwi Anggoro, Muhammad Hanif Dzikri Wibawa, Moch Zaenal Fathoni, 2017, Pembuatan Briket Arang dari Campuran Tempurung Kelapa dan Serbuk gergaji Kayu Sengon, *Teknik*, 38, 2, 76-80 https://doi.org/10.14710/teknik.v38i2.13985

[6] Esmar Budi, 2017, Pemanfaatan Briket Arang Tempurung Kelapa Sebagai Sumber Energi Alternatif, *Sarwahita*, 14, 1, 81-84 https://doi.org/10.21009/sarwahita.141.10

[7] Dimas Rahardian Aji Muhammad, Nur Her Riyadi Parnanto, Fanny Widadie, 2013, Kajian Peningkatan Mutu Briket Arang Tempurung Kelapa dengan Alat Pengering Tipe Rak Berbahan Bakar Biomassa, *Jurnal Teknologi Hasil Pertanian*, 6, 1, 23-26 https://doi.org/10.20961/jthp.v0i0.13500

[8] Gilar S Pambayun, Remigius YE Yulianto, M Rachimoellah, Endah MM Putri, 2013, Pembuatan karbon aktif dari arang tempurung kelapa dengan aktivator $ZnCl_2$ dan Na_2CO_3 sebagai adsorben untuk mengurangi kadar fenol dalam air limbah, *Jurnal Teknik ITS*, 2, 1, F116-F120 http://dx.doi.org/10.12962/j23373539.v2i1.2437

[9] Rinto Paputungan, Siti Nikmatin, Akhiruddin Maddu, Gustan Pari, 2018, Mikrostruktur Arang Aktif Batok Kelapa untuk Pemurnian Minyak Goreng Habis Pakai, *Jurnal Keteknikan Pertanian*, 6, 1, 69-74

[10] Nor Ain, Rodiansono Rodiansono, Kamilia Mustikasari, 2019, Efek Temperatur, Tekanan dan Waktu Reaksi pada Hidrogenasi Asam Heksadekanoat Menjadi 1-Eksadekanol Menggunakan Katalis Ru-Sn(3,0)/C, *Jurnal Kimia Sains dan Aplikasi*, 22, 4, 112-122 https://doi.org/10.14710/jksa.22.4.112-122

[11] Esther Bailón-García, Francisco J. Maldonado-Hódar, Agustín F. Pérez-Cadenas, Francisco Carrasco-Marín, 2013, Catalysts Supported on Carbon Materials for the Selective Hydrogenation of Citral, *Catalysts*, 3, 4, 853-877 https://doi.org/10.3390/catal3040853

[12] Rismawati Rasyid, Adrianto Prihartantyo, Mahfud Mahfud, Achmad Roesyadi, 2015, Hydrocracking of Calophyllum inophyllum oil with non-sulfide CoMo catalysts, *Bulletin of Chemical Reaction Engineering & Catalysis*, 10, 1, 61-69 https://doi.org/10.9767/bcrec.10.1.6597.61-69

[13] Mothi Krishna Mohan, KR Sunajadevi, Nobi K Daniel, Soumya Gopi, Sugunan Sugunan, Nikhil Chandra Perumparakunnel, 2018, Cu/Pd Bimetallic Supported on Mesoporous TiO2 for Suzuki Coupling Reaction, *Bulletin of Chemical Reaction Engineering & Catalysis*, 13, 2, 286-294 https://doi.org/10.9767/bcrec.13.2.1393.286-294

[14] Andrii Kostyniuk, David Key, Masikana Mdleleni, 2019, Effect of Fe-Mo promoters on HZSM-5 zeolite catalyst for 1-hexene aromatization, *Journal of Saudi Chemical Society*, 23, 5, 612-626 https://doi.org/10.1016/j.jscs.2018.11.001

[15] Wega Trisunaryanti, 2018, *Material Katalis dan Karakternya*, Gadjah Mada University Press, Yogyakarta

[16] Wega Trisunaryanti, 2002, Optimation of Time and Catalyst/Feed Ratio in Catalytic Cracking of Waste Plastics Fraction to Gasoline Fraction Using Cr/Natural Zeolite Catalyst, *Indonesian Journal of Chemistry*, 2, 1, 30-40 https://doi.org/10.22146/ijc.21930

[17] Saranya Ashokkumar, Vivekanandan Ganesan, Krishnamurthy K. Ramaswamy, Viswanathan Balasubramanian, 2018, Bimetallic Co–Ni/TiO2 catalysts for selective hydrogenation of cinnamaldehyde, *Research on Chemical Intermediates*, 44, 11, 6703-6720 https://doi.org/10.1007/s11164-018-3517-7

[18] Setijo Bismo, A. Azhariyah, Astrini Pradyasti, 2017, Potensi Karbon Aktif sebagai Penyangga Katalis Dekomposisi Ozon, *Seminar Nasional Integrasi Proses 2017*, Cilegon

[19] Upita Septiani, Mega Gustiana, Safni, 2015, Pembuatan Dan Karakterisasi Katalis TiO_2/Karbon Aktif dengan Metode Solid State, *Jurnal Riset Kimia*, 9, 1, 34 https://doi.org/10.25077/jrk.v9i1.257

[20] E Taer, T Oktaviani, R Taslim, R Farma, 2015, Karakterisasi Sifat Fisika Karbon Aktif Tempurung Kelapa Dengan Variasi Konsentrasi Aktivator Sebagai Kontrol Kelembaban, *Prosiding Seminar Nasional Fisika (E-Journal) SNF2015*

[21] Vivek Sheel Jaswal, Avnish Kumar Arora, Joginder Singh, Mayank Kinger, Vishnu Dev Gupta, 2014, Synthesis and characterization of chromium oxide nanoparticles, *Oriental Journal of Chemistry*, 30, 2, 559-566 http://dx.doi.org/10.13005/ojc/300220

[22] F Farzaneh, M Najafi, 2011, Synthesis and characterization of Cr_2O_3 nanoparticles with triethanolamine in water under microwave irradiation, *Journal of Sciences Islamic Republic of Iran*, 22, 4, 329-333

[23] Vidyanova Anggun Mentari, Gewa Handika, Seri Maulina, 2018, Perbandingan Gugus Fungsi dan Morfologi Permukaan Karbon Aktif dari Pelepah Kelapa Sawit Menggunakan Aktivator Asam Fosfat (H3PO4) dan Asam Nitrat (HNO3), *Jurnal Teknik Kimia USU*, 7, 1, 16-20 https://doi.org/10.32734/jtk.v7i1.1629

[24] Farhad Rahmani, Mohammad Haghighi, Majed Amini, 2015, The beneficial utilization of natural zeolite in preparation of Cr/clinoptilolite nanocatalyst used in CO2-oxidative dehydrogenation of ethane to ethylene, *Journal of Industrial and Engineering Chemistry*, 31, 142-155 https://doi.org/10.1016/j.jiec.2015.06.018

[25] Sen Tian, Xuemei Ye, Yaping Dong, Wu Li, Bo Zhang, Bo Li, Haitao Feng, 2019, Production and Characterization of Chromium Oxide (Cr_2O_3) via a Facile Combination of Electrooxidation and Calcination, *International Journal of Electrochemical Science*, 14, 8805-8818 https://doi.org/10.20964/2019.09.21

[26] Zainal Fanani, Dedi Rohendi, Tri Kurnia Dewi, 2016, Preparation and Characterization of Cr/Activated Carbon Catalyst from Palm Empty Fruit Bunch, *IJFAC (Indonesian Journal of Fundamental and Applied Chemistry)*, 1, 2, 35-41 http://dx.doi.org/10.24845/ijfac.v1.i2.35

[27] M. A. Lillo-Ródenas, D. Cazorla-Amorós, A. Linares-Solano, 2003, Understanding chemical reactions between carbons and NaOH and KOH: An insight into the chemical activation mechanism, *Carbon*, 41, 2, 267-275 https://doi.org/10.1016/S0008-6223(02)00279-8

[28]J. A. Melero, A. García, M. Clavero, 2011, 15 - Production of biofuels via catalytic cracking, in: R. Luque, J. Campelo, J. Clark (Eds.) *Handbook of Biofuels Production*, Woodhead Publishing, https://doi.org/10.1533/9780857090492.3.390

[29]Wega Trisunaryanti, Triyono Triyono, Denty Fibirna A, 2003, Preparation of Ni-Mo/Mordenite Catalysts under the Variation of Mo/Ni Ratio and Their Characterizations for Stearic Acid Conversion, *Indonesian Journal of Chemistry*, 3, 2, 80-90 https://doi.org/10.22146/ijc.21890

[30]Alexander Weinert, Alexander Reichhold, Peter Bielansky, Christoph Schönberger, Bettina Schumi, 2011, Bio-Gasoline from Jatropha Oil: New Applications for the FCC-Process, *10th International Conference on Circulating Fluidized Beds and Fluidization Technology - CFB-10*

[31] S. A. P. da Mota, A. A. Mancio, D. E. L. Lhamas, D. H. de Abreu, M. S. da Silva, W. G. dos Santos, D. A. R. de Castro, R. M. de Oliveira, M. E. Araújo, Luiz E. P. Borges, N. T. Machado, 2014, Production of green diesel by thermal catalytic cracking of crude palm oil (Elaeis guineensis Jacq) in a pilot plant, *Journal of Analytical and Applied Pyrolysis*, 110, 1-11 https://doi.org/10.1016/j.jaap.2014.06.011

[32]Xianhui Zhao, Lin Wei, Shouyun Cheng, James Julson, 2015, Optimization of catalytic cracking process for upgrading camelina oil to hydrocarbon biofuel, *Industrial Crops and Products*, 77, 516-526 https://doi.org/10.1016/j.indcrop.2015.09.019